Mass Spectrometry
DOI: 10.5702/massspectrometry.A0144
Vol. 13 (2024), A0144

Original Article

Mobilize a Proton to Transform the Collision-Induced Dissociation Spectral Pattern of a Cyclic Peptide

Takemichi Nakamura*,[1], Yayoi Hongo†,[1], and Ken-ichi Harada[2]

[1]*Molecular Structure Characterization Unit, RIKEN Center for Sustainable Resource Science, 2–1 Hirosawa, Wako, Saitama 351–0198, Japan*
[2]*Faculty of Pharmacy, Meijo University, 150 Yagotoyama, Tempaku, Nagoya 468–8503, Japan*

The collision-induced dissociation (CID) behaviors of protonated molecules of anabaenopeptins, a group of cyanobacterial cyclic peptides, were investigated in detail using liquid chromatography-tandem mass spectrometry. Although anabaenopeptin A and B share a macrocyclic peptide structure, they give strikingly different fragmentation patterns; the former gives a variety of product ions including cleavages in the cyclic peptide structure, which is useful for structural analysis; whereas the latter gives far fewer product ions and no fragmentation in the cyclic moiety. Energy-resolved CID experiments clarified the mechanism behind the striking difference attributable to the difference in exocyclic amino acid residues, Tyr or Arg. The guanidino group in Arg-containing analogue, anabaenopeptin B, should be by far the most preferred protonation site; the proton would be sequestered at the guanidino group in the protonated molecule, with the lack of proton mobility prohibiting opening of the charge-directed fragmentation channels in the cyclic moiety. Enzymatic hydrolysis of the guanidino group to give citrullinated-anabaenopeptin B restored proton mobility. The fragmentation pattern of the citrullinated peptide became almost identical to that of anabaenopeptin A. The observed fragmentation behaviors of these cyclic peptides were consistent with those of linear peptides, which have been well understood based on the mobile proton model.

Please cite this article as: Mass Spectrom (Tokyo) 2024; 13(1): A0144

Keywords: tandem mass spectrometry, fragmentation, mobile proton, energy-resolved CID, anabaenopeptin

(Received November 30, 2023; Accepted February 5, 2024; advance publication released online February 17, 2024)

INTRODUCTION

Modern liquid chromatography-mass spectrometry (LC-MS) instruments are mainly designed for use with an electrospray ionization (ESI) source,[1,2] which gives minimal fragmentation of analyte ions.[3,4] Consequently, many of the current LC-MS instruments also have tandem mass spectrometry (MS/MS) capability to allow observation of product ions that provides structural information regarding ESI-generated precursor ions.[5] The LC-(ESI)MS/MS technology has evolved since the 1990s.[6] Initially, the technology was extensively used in the field of proteomics due to its sensitivity and versatility for application to various mixtures.[7] In a typical procedure, proteolytic peptides are separated by LC and transferred to an ESI source, followed by MS/MS, in which protonated peptides are selected as precursor ions and then fragmented by low-energy collision-induced dissociation (CID).[6,8] In general, protonated peptide molecules mainly give product ions known as b- and y-ions according to the peptide backbone cleavages.[9] Although rather limited fragmentations have been observed in low-energy CID experiments, such limited information is often enough for the identification of peptides in proteomic applications in which the sequence databases are available for searching candidate peptide sequences.[10]

Following its successful application in the field of proteomics, LC-MS/MS quickly became a popular method for structural characterization in many fields, including natural product chemistry,[11] where it is often the only practical method for characterizing limited amounts of samples.[12–14] However, in contrast to the peptide identification in proteomics, structural characterization and identification of diverse organic molecules is a much more complicated and difficult task. In cases where very large chemical spaces of organic compounds need to be considered, the amount of information that can be obtained through a few MS/MS

*Correspondence to: Takemichi Nakamura, *Molecular Structure Characterization Unit, RIKEN Center for Sustainable Resource Science, 2–1 Hirosawa, Wako, Saitama 351–0198, Japan*, e-mail: takemi@a.riken.jp
†Present affiliation: Yayoi Hongo, Okinawa Institute of Science and Technology Graduate University, 1919–1 Tancha, Onna-son, Kunigami, Okinawa 904–0495, Japan

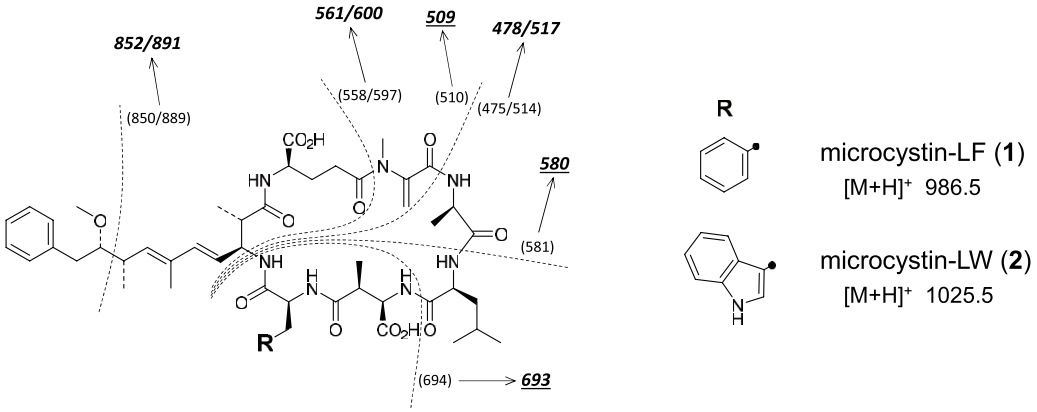

Fig. 1. The fragmentation patterns commonly observed in the CID spectra of protonated molecules from microcystin-LF (**1**) and microcystin-LW (**2**) are summarized based on the previous report.[22] The numbers in parentheses beside each dashed line are nominal masses corresponding to the side of each formal cleavage site on the chemical structures of **1** and **2**. The italicized numbers are nominal masses of actual fragment ions that were generated with hydrogen rearrangement(s). The underlined numbers are masses common in **1** and **2**, whereas the masses shown before/after slash signs are those shifted by 39 Da, which is the mass difference attributable to the different R groups in **1** and **2**. CID, collision-induced dissociation.

experiments on an unknown molecule would simply be insufficient for the structural elucidation of a medium-sized molecule from scratch.[15,16] On the other hand, once a chemical structure has been established by means of any method, including NMR, X-ray, *etc*., the structures of homologous compounds may be successfully characterized by LC-MS/MS.[17–20] In other words, successful characterization of natural products often relies on known structure(s) that can be used as a template.

The case of microcystins, a group of cyanobacterial cyclic peptides, is one such example.[21,22] As many of natural cyclic peptides are resistant to protease or peptidase, and have unique structural features including unusual amino acid residues, structure elucidation would become complicated processes. However, once the structure of a key compound has been established, homologous compounds could be characterized by LC-MS/MS. For example, based on the structure and MS/MS fragmentation pattern of microcystin-LF (**1**), the structure of microcystin-LW (**2**) was characterized rather quickly by interpreting very similar fragmentation patterns.[22] Fragment ions were observed either at the same *m/z* or at the position shifted by the difference of molecular masses as shown in Fig. 1.

Interestingly, similar structures do not always give similar fragmentation patterns. The case of another group of cyanobacterial cyclic peptides, anabaenopeptins,[23] is such an example. Although the difference between anabaenopeptin A (**3**) and B (**4**) is only a single amino acid residue as in the case of **1** and **2**, the fragmentation patterns observed in the CID spectra of **3** and **4** showed a striking difference.[24] The $[M+H]^+$ of **3** gave an information-rich product ion spectrum attributable to the peptide bond cleavages inside the cyclic peptide structure, whereas **4** only gave a product ion corresponding to loss of the exocyclic part (*m/z* 637) except for a couple of water losses. With no cleavages inside the cyclic structure, the fragmentation pattern of **4** was very poor in terms of structural information. In the previous study, it was demonstrated that the interior of the cyclic part of **4** can be further characterized by analyzing the second-generation product ion from *m/z* 637.[24] However, it remained unclear why the product ion spectra of protonated molecules of two compounds showed such an intriguing difference.

In the present study, we reinvestigated the MS/MS fragmentation behavior of anabaenopeptins. The objective of the study was 1) to understand why the similar structures show such different fragmentation patterns and 2) to explore whether there is any way to transform the fragmentation pattern of **4** into an "information-rich" pattern, based on our understanding of the underlying mechanisms. Our experiments revealed that proton mobility plays a key role in the fragmentation behaviors of the cyclic peptides, as we describe below.

EXPERIMENTAL

Materials

Anabaenopeptin A, B, and C were isolated from *Anabaena flos-aquae*, as reported previously.[23] Methanolic solutions were prepared from dried stock samples for the analysis. Protein arginine deiminase 4 (PAD4, human recombinant, 0.71 mg/mL in buffer solution) was purchased from Cayman Chemical Co. (Ann Arbor, MI, USA).

Preparation of citrullinated-anabaenopeptin B

The guanidino group of arginine-containing peptide was converted to a ureido-group by PAD4 digestion (citrullination) according to the previously reported methods.[25,26] Briefly, 5 μL of methanolic solution of anabaenopeptin B (*ca*. 1 mg/mL) was diluted with 50 μL of 100 mM Tris–HCl buffer (pH 7.5, containing 10 mM $CaCl_2$ and 2 mM dithiothreitol), and then 2.5 μL of PAD4 solution (1.78 μg enzyme) was added. The reaction mixture was incubated for 14.5 h at 37°C and then quenched with a 10-fold volume of 0.1% aqueous formic acid and stored in a freezer (−25°C) until analyzed by LC-MS/MS.

LC-MS/MS data acquisition and processing

All data were acquired by using a Synapt G2 quadrupole/time-of-flight (Q-TOF) tandem mass spectrometer (Waters Co., Manchester, UK) equipped with an Acquity UPLC system (Waters) and an ESI source. Samples were injected into a reversed-phase column (ACQUITY UPLC BEH C18 1.7 μm, 2.1×50 mm, at 25°C) and eluted with an isocratic solvent system (solvent A: 0.1% formic acid in water; solvent B: acetonitrile; 30% B) at a flow rate of 0.2 mL/min for short

LC-MS/MS runs. The ions generated at positive ESI capillary (3 kV) under atmospheric pressure went into the vacuum system through the sampling cone (15 V). The ions were transferred to the quadrupole mass analyzer for isolation of precursor ions of interests (*i.e.*, the protonated molecules of analytes). The isolated precursor ions were subjected to low-energy CID with Ar (99.9999%, 0.4 mL/min) at the trap collision cell (2.5×10^{-2} mbar). Ions went through the collision cell and the following ion optics were mass analyzed at the orthogonal TOF analyzer for the recording of a high-resolution (approx. 20,000 FWHM) externally calibrated product ion spectrum in each second. In post-run data processing, a few spectra at the retention time of each analyte were combined and converted to a centroid spectrum. A known-mass peak (typically the precursor ion peak) in each combined spectrum was used as an internal lock mass for recalibration to ensure ppm-level mass accuracy.

Energy-resolved CID data acquisition and processing

In the LC-MS/MS data acquisition procedure described above, collision energies applied at the trap cell were stepped from 2 V through 50 V (in 2 V steps for 1+ ions) or 1 V through 25 V (in 1 V steps for 2+ ions) in repeated runs for energy-resolved CID experiments. The product ion spectrum obtained at each collision energy was converted to a centroid peak list and used for calculating CID efficiency curves as follows: First, all the peak intensities from *m/z* 50 (the lower end of the recorded mass range) through the A+3 isotopic peak of 1+ precursor ions were added to obtain the total ion intensity in each spectrum. The intensity of 1+ precursor ions in each spectrum was calculated by adding the intensities of the monoisotopic $[M+H]^+$ peak and the isotopic peaks up to the A+3 position. The intensity of 2+ precursor ions in each spectrum was calculated by adding the peak intensities in the *m/z* range between 0.25 u below to 1.75 u above of the *m/z* value corresponding to the monoisotopic $[M+2H]^{2+}$ peak. Each product ion spectra from doubly charged precursor ions was manually inspected to confirm no major product ion peaks (>1% of the total ion intensity) were present in the range of 2+ precursor ions. The sum of product ion intensities in each spectrum was obtained by subtracting the intensity of precursor ions from the total ion intensity. Finally, the sum of the product ion intensities was divided by the total ion intensity to calculate the CID efficiency at each collision energy for plotting.

RESULTS AND DISCUSSION

In this study, we re-examined the low-energy CID product ion spectra of **3** and **4** by using a Q-TOF tandem mass spectrometer. In the LC–ESI mass spectra of **3** and **4**, both $[M+H]^+$ ions and some doubly charged ions were observed (Supplementary Fig. S1). Initially, we focused on the fragmentation behavior of the $[M+H]^+$ ions simply because our first goal was to understand why the singly protonated molecules of these compounds gave such different spectral patterns in the previous study.[24] The CID product ion spectra from the $[M+H]^+$ of **3** and **4** are shown in Fig. 2; the assignments of major product ions shown on the structures were supported by the accurate mass measurements (Supplementary Tables S1 and S2).

The previously reported striking difference between **3** and **4** was reproduced in the current study (*i.e.*, no cleavages were observed in the cyclic peptide part of **4** [Fig. 2]). Interestingly, in addition to *m/z* 637, which corresponded to the intact cyclic part, strong ions at *m/z* 201 and 175 were observed in the CID spectrum of **4**. These lower mass ions were not reported in the previous study using an ion trap mass spectrometer,[24] presumably due to the lower-mass cutoff of the ion trap. Based on the accurate mass measurements (Table S2), *m/z* 201 and 175 were assigned to the fragment ions attributable to the arginine part as the putative ion structures shown in Fig. 2, panel B.

Observation of the arginine-part fragment ions led us to conjecture that the different behaviors of **3** and **4** could be understood based on the mobile proton model.[27] This model provided a framework for understanding both the surface-induced and collision-induced fragmentation behavior of protonated organic molecules.[28,29] It has been well established that the fragmentation behavior of linear peptide ions depends on the presence or absence of mobile protons, which can be affected by several factors, including the presence or absence of Arg residues. Under ESI conditions, peptides containing an Arg residue are considered to be protonated at the highly basic guanidino group. Because the proton binds to the guanidino group strongly and is not mobile, it cannot migrate to the peptide backbone to facilitate bond cleavages with charge-directed mechanisms. Consequently, the internal energy deposition required for fragmenting Arg-containing peptides is higher than that for Arg-free peptides. Because such differences in energy requirement can be visualized in fragmentation efficiency curves obtained by energy-resolved experiments,[29] we ran energy-resolved CID MS/MS experiments on anabaenopeptins to compare the fragmentation efficiency curve for each analogue. As shown in Fig. 3, the fragmentation efficiency curve for **4** was clearly shifted to the right from that for **3** (*i.e.*, the energy requirement for fragmentation of the Arg-containing analogue (**4**) was much higher than that of **3**). Because this observation was consistent with the mobile proton model, we hypothesized that the lack of fragmentation in the cyclic peptide part of **4** was attributable to a lack of proton mobility. This hypothesis could be tested by modifying the guanidino group in Arg to reduce proton affinity so that the proton mobility would increase.

A few derivatization/modification methods have been used for characterization of Arg-containing peptides by mass spectrometry. Such methods include the formation of pyrimidine derivative with acatylacetone[30] or malondialdehyde,[31] chemical conversion of Arg to ornithine residue,[32] and enzymatic conversion of Arg to citrulline (Cit) residue by peptidyl arginine deiminase.[26,33] To modify the Arg residue of **4**, we applied the enzymatic conversion method, which can be carried out under very mild conditions. The proton affinity of the ureido group generated by the conversion should be much lower than that of the highly basic guanidino group, and hence the proton mobility should be increased. To verify this, we ran energy-resolved CID MS/MS experiments on citrullinated-anabaenopeptin B (**5**) obtained by the enzymatic digestion. In addition, we examined anabaenopeptin C (**6**), another naturally occurring anabaenopeptin[21] that has an exocyclic lysine residue instead of Tyr in **4** or Arg in **5** as an additional reference.

The fragmentation efficiency curve for **5** (Fig. 4) looked quite similar to that for **3** (Fig. 3); the curve clearly demonstrated that the fragmentation of **5** requires much less energy

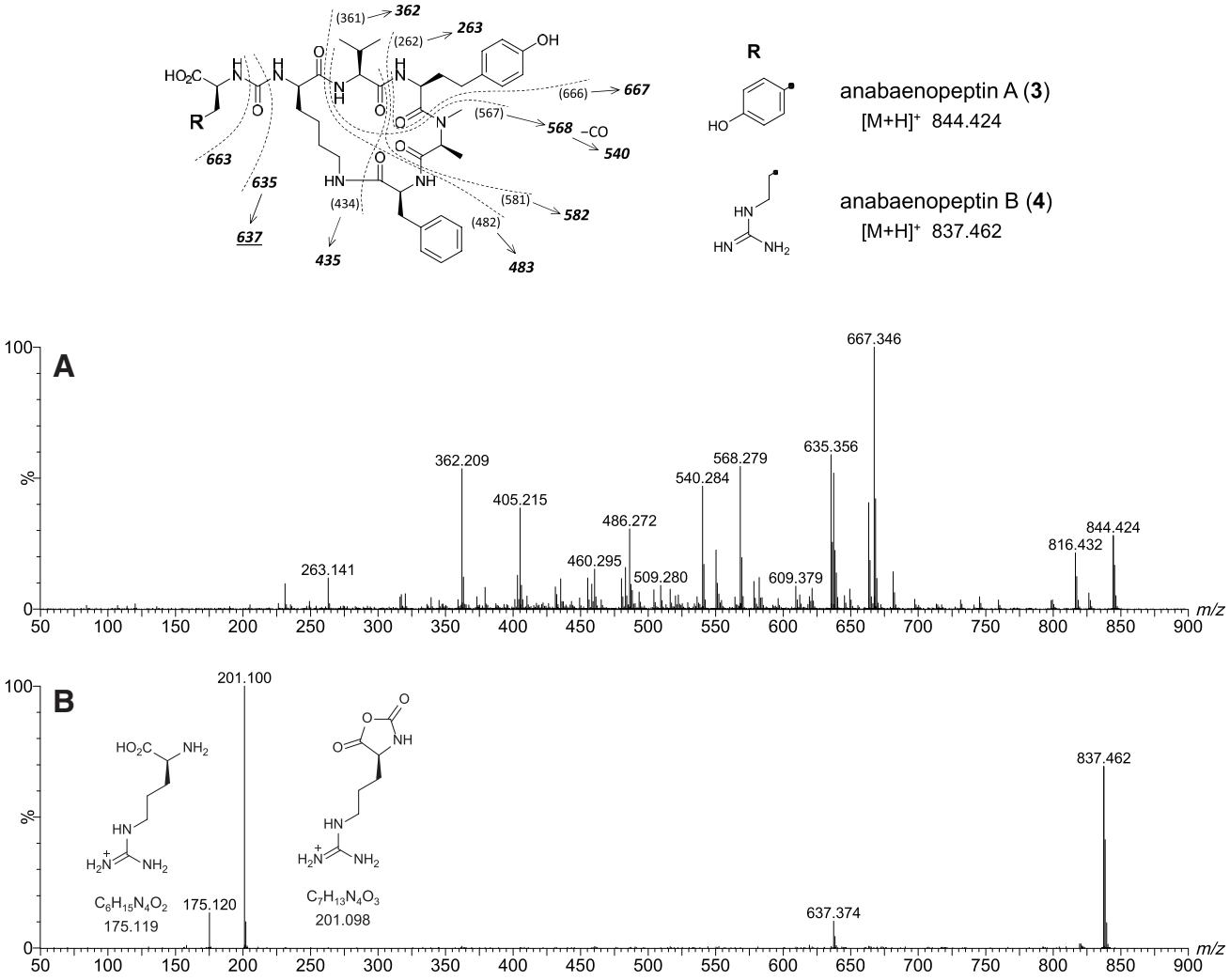

Fig. 2. Product ion spectra from the protonated molecules of anabaenopeptin A (**3**) and B (**4**) acquired at a 40 eV laboratory-frame collision energy with the assignments of characteristic fragment ions. The product ion spectrum of **3** (panel A) shows fragmentations attributable to various cleavages in the cyclic peptide structure. The numbers in parentheses beside each dashed line are nominal masses corresponding to the side of each formal cleavage site on the chemical structure for **3**. The italicized numbers are nominal masses of actual fragment ions that were generated with hydrogen rearrangement(s). The fragment ion attributable to the intact cyclic peptide part (*m/z* 637) was also observed in the product ion spectrum of **4** (panel B). The spectrum data files are available in J-STAGE Data. https://doi.org/10.50893/data.massspectrometry.25232693

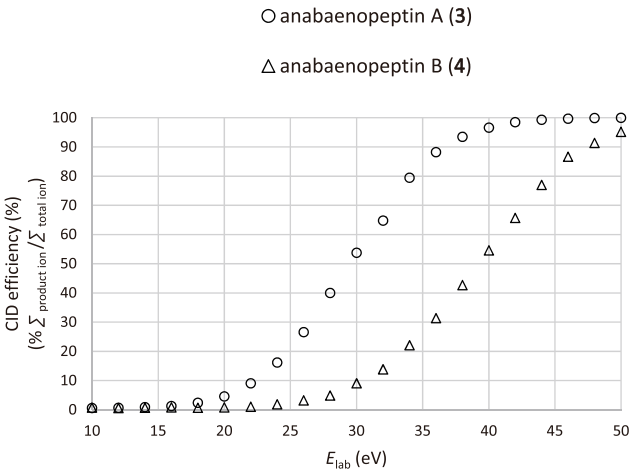

Fig. 3. Fragmentation efficiency curves for anabaenopeptin A (**3**) and anabaenopeptin B (**4**) obtained by energy-resolved CID MS/MS experiments. CID, collision-induced dissociation; MS/MS, tandem mass spectrometry.

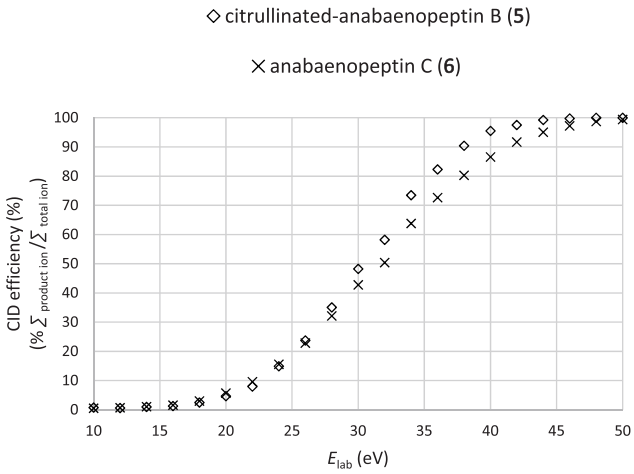

Fig. 4. Fragmentation efficiency curves for citrullinated-anabaenopeptin B (**5**) and anabaenopeptin C (**6**) obtained by energy-resolved CID MS/MS experiments. CID, collision-induced dissociation; MS/MS, tandem mass spectrometry.

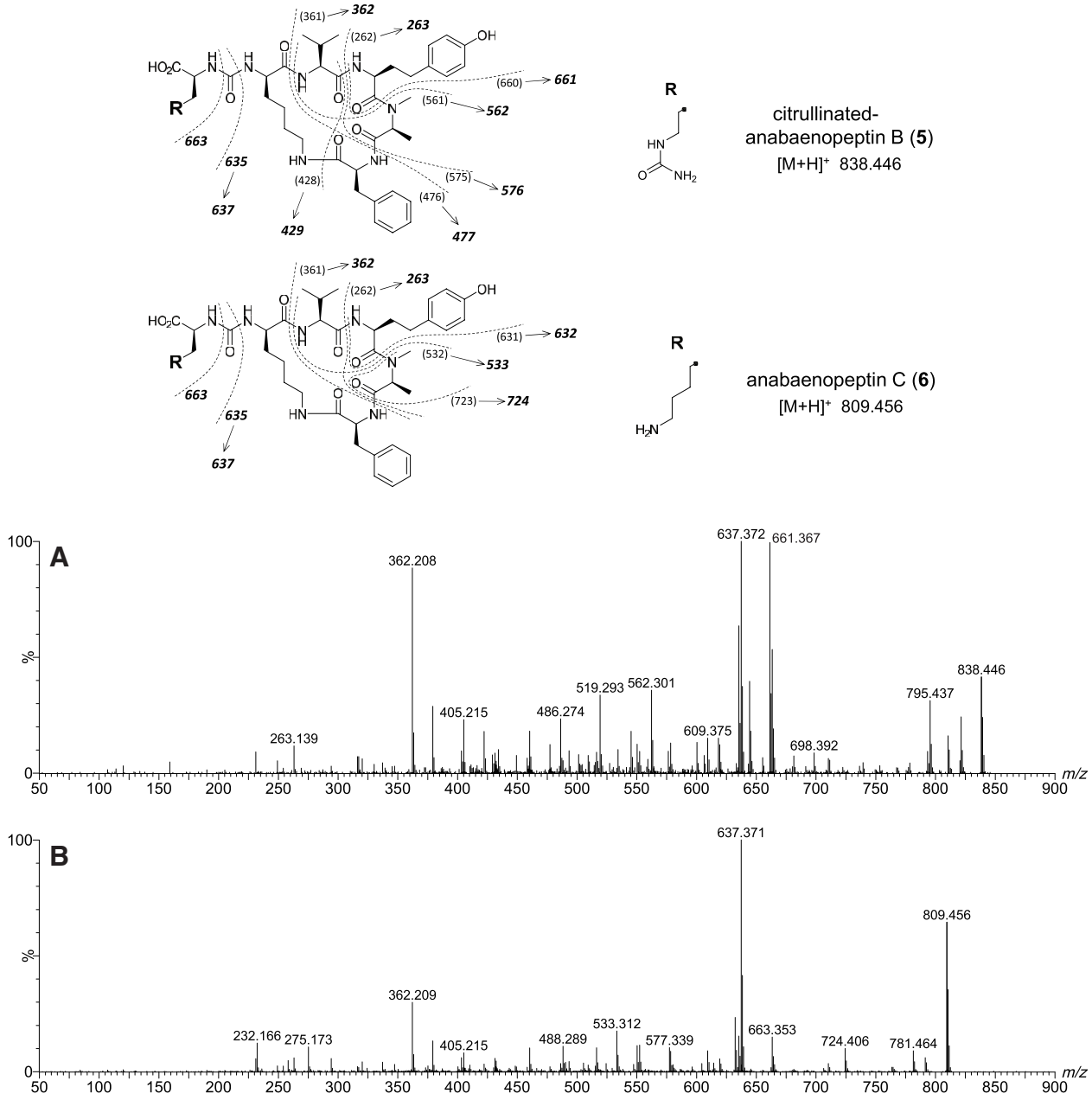

Fig. 5. Product ion spectra from the protonated molecules of citrullinated-anabaenopeptin B (**5**) (panel A) and anabaenopeptin C (**6**) (panel B) acquired at a 40 eV laboratory-frame collision energy with the assignments of characteristic fragment ions supported by the accurate mass measurements (Supplementary Tables S3 and S4). The numbers in parentheses beside each dashed line are nominal masses corresponding to the side of each formal cleavage site on the chemical structures. The italicized numbers are nominal masses of actual fragment ions that were generated with hydrogen rearrangement(s). The spectrum data files are available in J-STAGE Data. https://doi.org/10.50893/data.massspectrometry.25232763

compared to that of **4**, as expected. This observation could be explained by the mobile proton model, namely, the increased (or restored) proton mobility of $[M+H]^+$ of **5** facilitated the fragmentation under the CID conditions. The effect of proton mobilization was also clearly shown in the CID spectrum of **5** (Fig. 5, panel A). The appearance of the spectrum changed dramatically from that of **4**. The fragmentation pattern of **5**, which included many product ions attributable to the cleavages of the cyclic peptide part, looked quite similar to the fragmentation pattern of **3**; indeed, the spectral pattern was improved by the removal of the guanidino group and restoration of proton mobility.

Interestingly, although the fragmentation efficiency curve for **6** (Fig. 4) also showed a much smaller energy requirement compared to that for **4**, the curve appeared to be a little less steep or slightly shifted towards the right compared to the curves for **3** and **5**. The difference is likely attributable to the somewhat limited proton mobility caused by the Lys residue.[27,29] The appearance of the CID spectrum of **6** (Fig. 5, panel B) also suggested that the fragmentation of the Lys-containing analogue was a little more difficult than that of **3** or **5** but much easier than that of the Arg-containing analogue, **4**. Some of the characteristic fragmentation in the cyclic peptide part was still visible in the CID spectrum of **6** with relatively low intensities.

Since it was demonstrated that the lack of proton mobility limited the fragmentation from $[M+H]^+$ of anabaenopeptin B (**4**), we have also looked at the fragmentation behaviors of

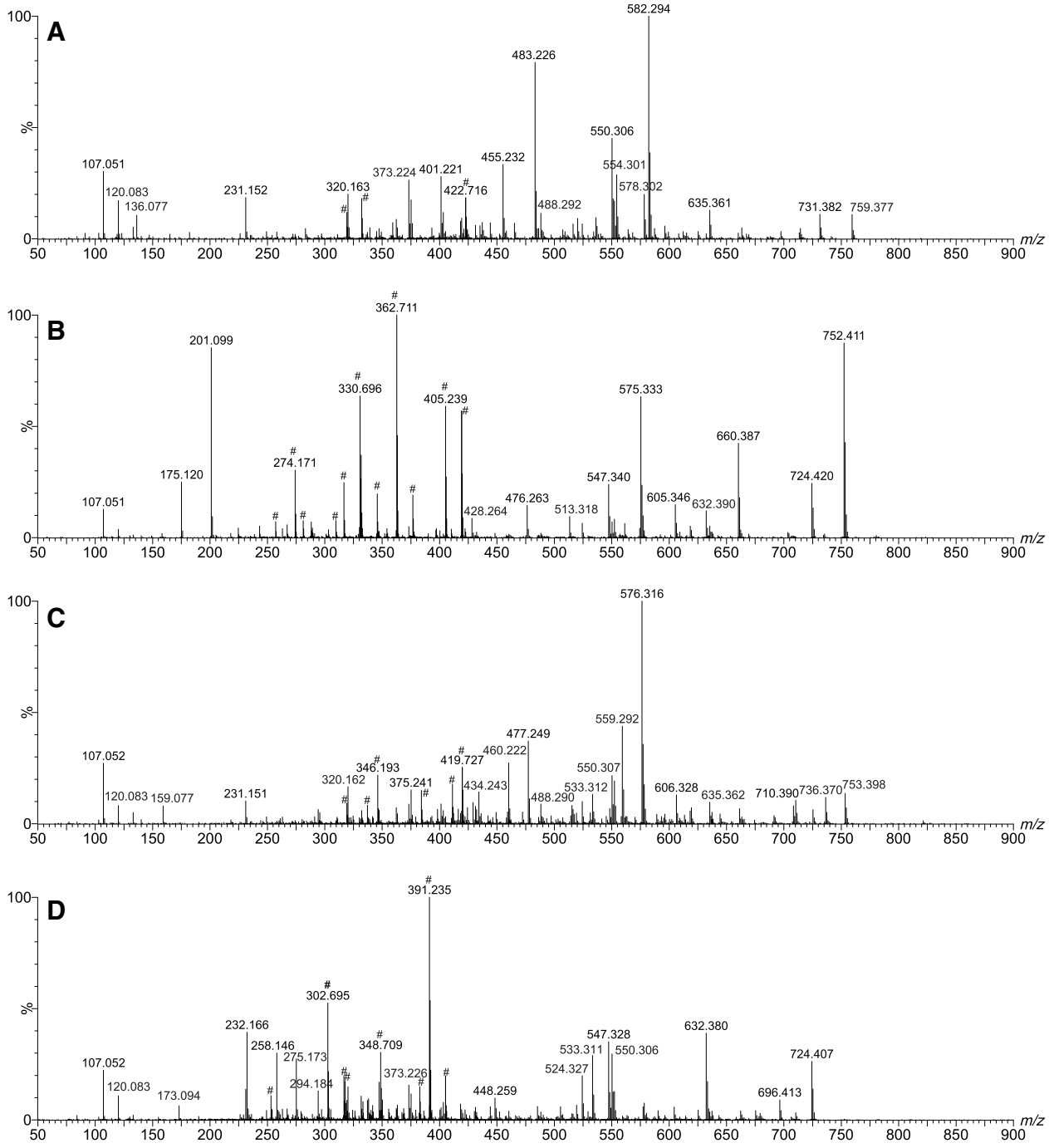

Fig. 6. Product ion spectra from the $[M+2H]^{2+}$ ions of anabaenopeptin A (**3**) (panel A), anabaenopeptin B (**4**) (panel B), citrullinated-anabaenopeptin B (**5**) (panel C), and anabaenopeptin C (**6**) (panel D), acquired at a 20 eV laboratory-frame collision energy. Doubly charged ions are marked with #. The spectrum data files are available in J-STAGE Data. https://doi.org/10.50893/data.massspectrometry.25232774

the doubly protonated molecules of **4** and other anabaenopeptin analogues. In contrast to the striking differences in the CID spectra from $[M+H]^+$ ions of anabaenopeptins A, B, citrullinated-B, and C, the $[M+2H]^{2+}$ ions of these compounds showed more or less extensive fragmentations (Fig. 6). The onsets of the fragmentation efficiency curves were rather close to each other (Fig. 7). Such behaviors of the doubly charged cyclic peptide ions were consistent with the behaviors of linear peptide ions explained by the mobile proton model.[27] The model explains well the mechanism behind the fact that multiply protonated tryptic peptides with C-terminal Arg residue tend to give more fragment ions compared to singly protonated counterparts under low-energy CID conditions.[9] In a doubly protonated Arg-peptide, the first proton is sequestered at the Arg residue but the second proton is mobile and available to open various charge-directed fragmentation channels. Consequently, sequencing of linear peptides is often carried out by analyzing product ion spectra from multiply protonated precursor ions. However, the analysis of product ion spectra from cyclic peptides can be much more complicated than that of linear peptides. Therefore,

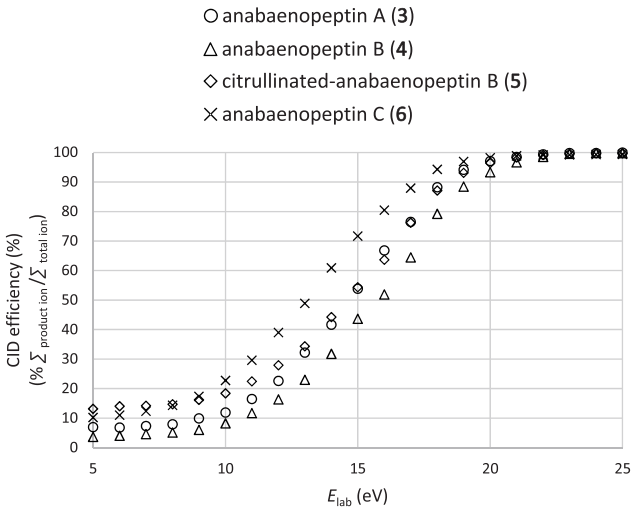

Fig. 7. Fragmentation efficiency curves for the $[M+2H]^{2+}$ ions of anabaenopeptin A (**3**), anabaenopeptin B (**4**), citrullinated-anabaenopeptin B (**5**), and anabaenopeptin C (**6**). CID, collision-induced dissociation.

we looked at the product ion spectra from $[M+2H]^{2+}$ of anabaenopeptins in detail.

In the case of anabaenopeptins, it turned out that the interpretation of product ion spectra from $[M+2H]^{2+}$ of the cyclic peptides was not as easy as the interpretation of those from $[M+H]^{+}$ ions. However, we have managed to assign the characteristic product ions from the $[M+2H]^{2+}$ ions as shown in Fig. 8. First, some strong secondary neutral losses and doubly charged product ions were observed in the product ion spectra from the doubly protonated cyclic peptides. The neutral losses and doubly charged product ions complicated the spectral interpretation. In addition, although some of the fragmentation channels governed by mobile protons were considered to be restored by adding an extra proton to anabaenopeptin B, the observed fragmentation pattern from the Arg-containing cyclic peptide was somewhat different from the fragmentation patterns from the Arg-free analogues. As shown in Fig. 8, a few product ions not containing the side-chain R residues were observed in the product ion spectra from $[M+2H]^{2+}$ of anabaenopeptin A (**3**), citrullinated-B (**5**), and C (**6**). On the other hand, such product ions were missing in the product ion spectrum from $[M+2H]^{2+}$ of anabaenopeptin B (**4**) (*i.e.*, Arg-containing product ions dominated the product ion spectrum). Furthermore, the major doubly charged product ions from anabaenopeptin B (**4**) at *m/z* 362.711, 330.696, and 274.171 (Fig. 6, panel B) were assigned to Arg-containing product ions, namely, the doubly charged ions corresponding to the product ions at *m/z* 724.420, 660.387, and 547.340, respectively. It appears the additional (mobile) proton induced charge-directed fragmentation in the CID process while the proton on the Arg residue continued to be sequestered. Whether such characteristic of the Arg-containing cyclic peptide (**4**) helps structural characterization or not would depend on circumstances. However, if the structure of **4** was unknown, we can imagine that it would be rather difficult to characterize the Arg-containing peptide by using the CID-spectra of the Arg-free analogues as templates, since the fragmentation pattern of the doubly protonated Arg-peptide (**4**) was not very close to that of the doubly protonated Arg-free analogues. Therefore, for the purpose of structural characterization, it would be advantageous to take the previously mentioned enzymatic digestion strategy that allows the mobilization of a proton in singly charged precursor ions instead of looking at doubly protonated precursor ions.

CONCLUSIONS

The mobile proton model explained well why the fragmentation pattern of anabaenopeptin B (**4**) was completely different from those of the other anabaenopeptins. 1) Both the higher onset of the fragmentation efficiency curve and the smaller number of fragment ions from $[M+H]^{+}$ of **4**, the Arg-containing cyclic peptide, were a consequence of the lack of proton mobility; the lack of proton mobility prohibited the opening of the charge-directed fragmentation channels observed in other analogues. 2) The fragmentation of Arg-containing cyclic peptides may be facilitated by the restoration of proton mobility, which could be achieved by enzymatic conversion of the guanidino group into a ureido group with PAD4, as demonstrated in the case of conversion from **4** to the citrullinated analogue, **5**. The fragmentation of the Arg-containing peptide (**4**) can also be facilitated by the additional (mobile) proton in the doubly protonated precursor ions. However, the CID spectral pattern of the doubly protonated Arg-peptide was different from those of the doubly protonated Arg-free analogues. Obviously, in addition to the presence or absence of a mobile proton, the number of mobile protons in the precursor ions and/or the presence or absence of sequestered proton at the Arg-residue affected the CID spectral patterns of the analogous cyclic peptide structures.

It is an inconvenient reality that "analogous structures" do not always give similar CID spectral patterns; we cannot currently avoid this problem in the structural characterization process. However, our current results suggest that mechanistic considerations may help us to understand why fragmentation behavior changes so that we can find a way to transform the spectral patterns into preferable ones.

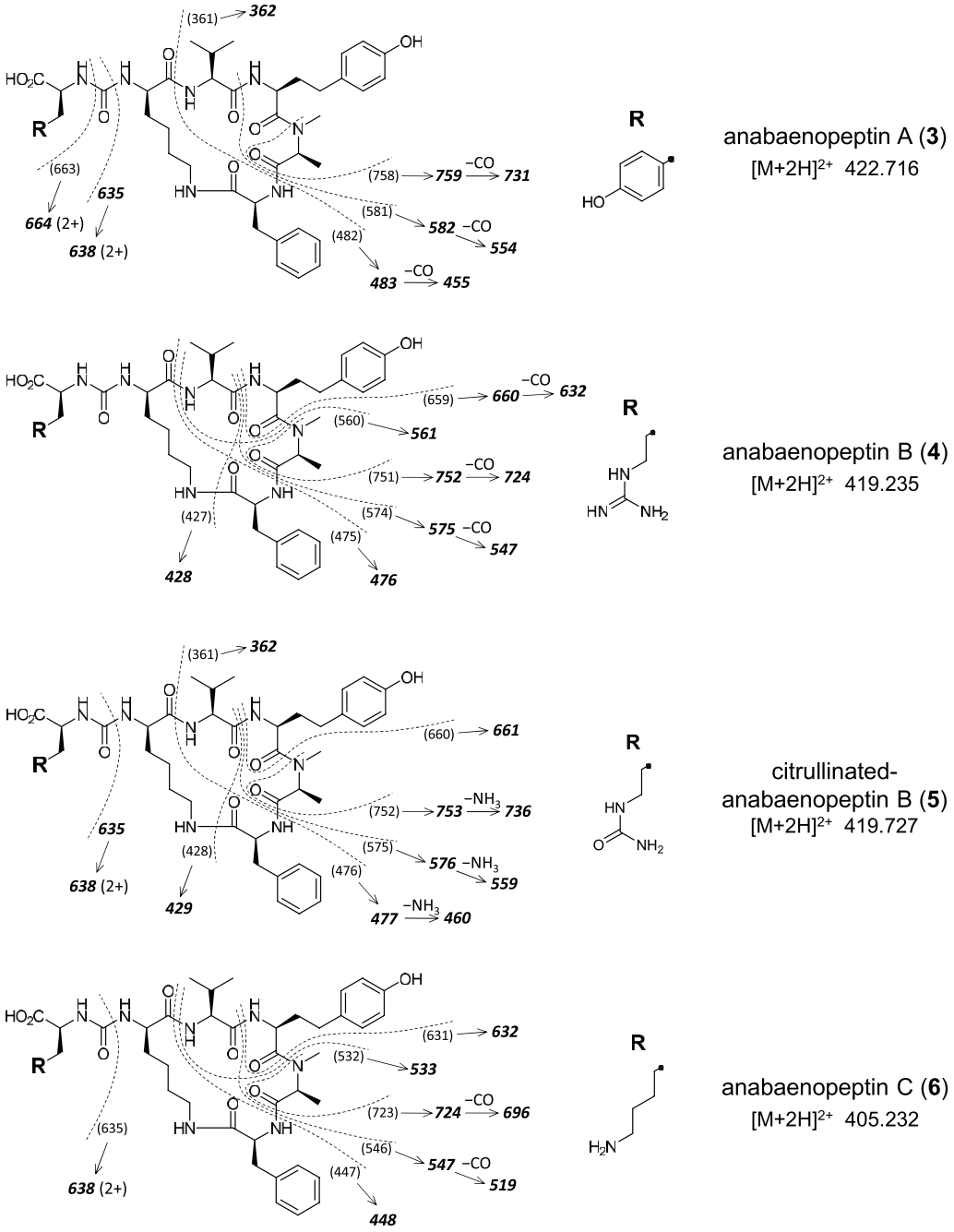

Fig. 8. Characteristic fragment ions from $[M+2H]^{2+}$ ions of anabaenopeptin analogues. The assignments were supported by the accurate mass measurements (Supplementary Tables S5 to S8). The numbers in parentheses beside each dashed line are nominal masses corresponding to the side of each formal cleavage site on the chemical structures. The italicized numbers are nominal masses of actual fragment ions that were generated with hydrogen rearrangement(s). The italicized numbers followed by (2+) are nominal masses corresponding to doubly charged product ions (a half of each number corresponds to the *m/z* of each doubly charged ion species).

ACKNOWLEDGMENTS

The authors thank Dr. Tsuyoshi Mayumi for helpful discussions regarding their previous ion-trap studies on various cyanobacterial cyclic peptides. This work was partly supported by MEXT/JSPS KAKENHI 25513011, 17K08262, and 21K05138.

DATA AVAILABILITY STATEMENT

In addition to the supplementary tables and figures, the spectral data in CSV format are deposited with the supporting information.

The spectrum data files are available in J-STAGE Data.

REFERENCES

1) R. D. Voyksner. Combining liquid chromatography with electrospray mass spectrometry. in *Electrospray Ionization Mass Spectrometry* (Ed: R. B. Cole), John Wiley & Sons, Inc., New York, 1997, pp. 323–341.
2) A. P. Bruins. Technologies for atmospheric-pressure ionization in LC–MS. in *The Encyclopedia of Mass Spectrometry Volume 8: Hyphenated Methods*, 1st Ed. (Ed: W. Niessen), Elsevier, Amsterdam, 2006, pp. 156–163.
3) R. B. Cody. Electrospray ionization mass spectrometry: History, theory, and instrumentation. in *Applied Electrospray Mass*

Spectrometry (Ed: A. K. G. B. N. Pramanik, M. L. Gross), Marcel Dekker, Inc., New York, 2002, pp. 1–104.

4) N. B. Cech, C. G. Enke. Electrospray ionization: How and when it works. in *The Encyclopedia of Mass Spectrometry Volume 8: Hyphenated Methods*, 1st Ed. (Ed: W. Niessen), Elsevier, Amsterdam, 2006, pp. 171–180.
5) T. Covey. Where have all the ions gone, long time passing? Tandem quadrupole mass spectrometers with atmospheric pressure ionization sensitivity gains since the mid-1970s. A perspective. *Rapid Commun. Mass Spectrom*. e9354, 2022.
6) J. R. Yates 3rd. Mass spectrometry and the age of the proteome. *J. Mass Spectrom*. 33: 1–19, 1998.
7) R. Aebersold, D. R. Goodlett. Mass spectrometry in proteomics. *Chem. Rev*. 101: 269–296, 2001.
8) S. A. McLuckey, D. E. Goeringer. Slow heating methods in tandem mass spectrometry. *J. Mass Spectrom*. 32: 461–474, 1997.
9) Y. Huang, J. M. Triscari, G. C. Tseng, L. Pasa-Tolic, M. S. Lipton, R. D. Smith, V. H. Wysocki. Statistical characterization of the charge state and residue dependence of low-energy CID peptide dissociation patterns. *Anal. Chem*. 77: 5800–5813, 2005.
10) M. A. Baldwin. Protein identification by mass spectrometry — Issues to be considered. *Mol. Cell. Proteomics* 3: 1–9, 2004.
11) J.-L. Wolfender, K. Hostettmann. Dereplication of flavonoids using multidimensional LC–MS techniques. in *The Encyclopedia of Mass Spectrometry Volume 8: Hyphenated Methods*, 1st Ed. (Ed: W. Niessen), Elsevier, Amsterdam, 2006, pp. 760–775.
12) J. Wang. Analysis of macrolide antibiotics, using liquid chromatography-mass spectrometry, in food, biological and environmental matrices. *Mass Spectrom. Rev*. 28: 50–92, 2009.
13) R. March, J. Brodbelt. Analysis of flavonoids: Tandem mass spectrometry, computational methods, and NMR. *J. Mass Spectrom*. 43: 1581–1617, 2008.
14) K. V. Sashidhara, J. N. Rosaiah. Various dereplication strategies using LC-MS for rapid natural product lead identification and drug discovery. *Nat. Prod. Commun*. 2: 193–202, 2007.
15) T. Kind, H. Tsugawa, T. Cajka, Y. Ma, Z. Lai, S. S. Mehta, G. Wohlgemuth, D. K. Barupal, M. R. Showalter, M. Arita, O. Fiehn. Identification of small molecules using accurate mass MS/MS search. *Mass Spectrom. Rev*. 37: 513–532, 2018.
16) R. M. Gathungu, R. Kautz, B. S. Kristal, S. S. Bird, P. Vouros. The integration of LC-MS and NMR for the analysis of low molecular weight trace analytes in complex matrices. *Mass Spectrom. Rev*. 39: 35–54, 2020.
17) W. M. Niessen. Fragmentation of toxicologically relevant drugs in positive-ion liquid chromatography–tandem mass spectrometry. *Mass Spectrom. Rev*. 30: 626–663, 2011.
18) M. Pulfer, R. C. Murphy. Electrospray mass spectrometry of phospholipids. *Mass Spectrom. Rev*. 22: 332–364, 2003.
19) J. Liu, R. Zhang, J. He, Y. Liu, J. Shi, Z. Abliz. The characteristic fragmentation and rearrangement reaction of cationized glucopyranosyloxybenzyl tartrates by tandem mass spectrometry. *J. Mass Spectrom*. 45: 824–828, 2010.
20) T. Cai, Z. Q. Guo, X. Y. Xu, Z. J. Wu. Recent (2000–2015) developments in the analysis of minor unknown natural products based on characteristic fragment information using LC–MS. *Mass Spectrom. Rev*. 37: 202–216, 2018.
21) K. Fujii, K. Sivonen, T. Nakano, K. Harada. Structural elucidation of cyanobacterial peptides encoded by peptide synthetase gene in *Anabaena* species. *Tetrahedron* 58: 6863–6871, 2002.
22) T. Mayumi, H. Kato, S. Imanishi, Y. Kawasaki, M. Hasegawa, K. Harada. Structural characterization of microcystins by LC/MS/MS under ion trap conditions. *J. Antibiot.* 59: 710–719, 2006.
23) K. Harada, K. Fujii, T. Shimada, M. Suzuki, H. Sano, K. Adachi, W. W. Carmichael. Two cyclic peptides, anabaenopeptins, a third group of bioactive compounds from the cyanobacterium *Anabaena flos-aquae* NRC 525-17. *Tetrahedron Lett*. 36: 1511–1514, 1995.
24) T. Mayumi, H. Kato, Y. Kawasaki, K. Harada. Formation of diagnostic product ions from cyanobacterial cyclic peptides by the two-bond fission mechanism using ion trap liquid chromatography/multi-stage mass spectrometry. *Rapid Commun. Mass Spectrom*. 21: 1025–1033, 2007.
25) P. L. Kearney, M. Bhatia, N. G. Jones, L. Yuan, M. C. Glascock, K. L. Catchings, M. Yamada, P. R. Thompson. Kinetic characterization of protein arginine deiminase 4: A transcriptional corepressor implicated in the onset and progression of rheumatoid arthritis. *Biochemistry* 44: 10570–10582, 2005.
26) K. Kubota, T. Yoneyama-Takazawa, K. Ichikawa. Determination of sites citrullinated by peptidylarginine deiminase using ^{18}O stable isotope labeling and mass spectrometry. *Rapid Commun. Mass Spectrom*. 19: 683–688, 2005.
27) V. H. Wysocki, G. Tsaprailis, L. L. Smith, L. A. Breci. Mobile and localized protons: A framework for understanding peptide dissociation. *J. Mass Spectrom*. 35: 1399–1406, 2000.
28) S. G. Summerfield, S. J. Gaskell. Fragmentation efficiencies of peptide ions following low energy collisional activation. *Int. J. Mass Spectrom. Ion Process*. 165–166: 509–521, 1997.
29) A. R. Dongré, J. L. Jones, Á. Somogyi, V. H. Wysocki. Influence of peptide composition, gas-phase basicity, and chemical modification on fragmentation efficiency: Evidence for the mobile proton model. *J. Am. Chem. Soc*. 118: 8365–8374, 1996.
30) P. A. Leclercq, L. C. Smith, D. M. Desiderio Jr. Modification, permethylation and mass spectrometry of arginine-containing oligopeptides at the 100 nanomolar level. *Biochem. Biophys. Res. Commun*. 45: 937–944, 1971.
31) A. Foettinger, A. Leitner, W. Lindner. Derivatisation of arginine residues with malondialdehyde for the analysis of peptides and protein digests by LC-ESI-MSMS. *J. Mass Spectrom*. 41: 623–632, 2006.
32) H. Kuyama, C. Nakajima, T. Nakazawa, O. Nishimura. Conversion of arginine to ornithine for improving the fragmentation pattern of peptides labeled with the N-terminal tris(2,4,6-trimethoxyphenyl) phosphonium group in tandem mass spectrometry. *Anal. Methods* 2: 1792–1797, 2010.
33) H. Kuyama, C. Nakajima, T. Nakazawa, O. Nishimura. Enzymatic conversion of arginine to citrulline for improving fragmentation of N^{α}-tris(2,4,6-trimethoxyphenyl)phosphonium-acetylated peptides by tandem mass spectrometry. *Anal. Methods* 3: 2829–2835, 2011.